Storage ring cross section measurements for electron impact ionization of Fe^{8+}

2016 J. Phys. B: At. Mol. Opt. Phys. 49 084006

(http://iopscience.iop.org/0953-4075/49/8/084006)

IOP Publishing Journal of Physics B: Atomic, Molecular and Optical Physics
J. Phys. B: At. Mol. Opt. Phys. **49** (2016) 084006 (8pp) doi:10.1088/0953-4075/49/8/084006

Storage ring cross section measurements for electron impact ionization of Fe^{8+}

M Hahn[1], A Becker[2], D Bernhardt[3], M Grieser[2], C Krantz[2], M Lestinsky[4], A Müller[3], O Novotný[1], M S Pindzola[5], R Repnow[2], S Schippers[3,6], K Spruck[3], A Wolf[2] and D W Savin[1]

[1] Columbia Astrophysics Laboratory, Columbia University, 550 West 120th Street, New York, NY 10027 USA
[2] Max-Planck-Institut für Kernphysik, Saupfercheckweg 1, D-69117 Heidelberg, Germany
[3] Institut für Atom- und Molekülphysik, Justus-Liebig-Universität Giessen, Leihgesterner Weg 217, D-35392 Giessen, Germany
[4] GSI Helmholtzzentrum für Schwerionenforschung, Planckstr. 1, D-64291 Darmstadt, Germany
[5] Auburn University, 2016 Allison Laboratory, Auburn, AL 36849 USA
[6] Physikalisches Institut, Justus-Liebig-Universität Giessen, Heinrich-Buff-Ring 16, D35392 Giessen, Germany

E-mail: mhahn@astro.columbia.edu

Received 27 October 2015, revised 25 January 2016
Accepted for publication 1 February 2016
Published 5 April 2016

Abstract

We have measured electron impact ionization (EII) for Fe^{8+} forming Fe^{9+} from below the ionization threshold to 1200 eV. These measurements were carried out at the TSR heavy ion storage ring. The objective of using a storage ring is to store the ion beam initially so that metastable levels decay, thereby allowing for measurements on a well-defined ground-level ion beam. In this case, however, some metastable levels were too long lived to be removed. We discuss several methods for quantifying the metastable fraction, which we estimate to be ~30%–40%. Although metastables remain problematic, the present storage ring work improves upon other experimental geometries by limiting the metastable contamination to only a few long-lived excited levels. We discuss some future prospects for obtaining improved measurements of Fe^{8+} and other ions with long-lived metastable levels.

Keywords: laboratory astrophysics, electron impact ionization, cross section, ion storage ring

1. Introduction

The Fe^{8+} ion is of particular interest for solar and stellar physics. In collisional ionization equilibrium this ion is most abundant at about 7×10^5 K [1]. For studies of the Sun, emission from this ion probes relatively cool structures in the solar corona. Several lines from this ion are observed by the EUV Imaging Spectrometer on the *Hinode* satellite and are useful temperature and density diagnostics [2, 3]. The 171.07 Å line is also the dominant contribution to the 171 Å bandpass of the atmospheric imaging assembly onboard the *Solar Dynamics Observatory* [4]. Lines at shorter wavelengths from this ion are observed in other stars by *Chandra* (e.g., [5]). Thus, more accurate data for Fe^{8+} would enable more precise diagnostics relevant for solar and stellar physics.

Because it is not practical to obtain experimental measurements for every astrophysically relevant ion, most data have come from theoretical calculations. Such calculations necessarily make approximations. In order to understand the consequent limitations of theory, these calculations must be compared with empirical reality. Measurements, though, are subject to various systematic uncertainties. One of the major sources of ambiguity for previous experiments is that the ion beams contained unknown populations of metastable ions. The measured collision cross sections are a weighted sum over those from the metastable and ground states. The primary advantage of storage-ring measurements is that storing the ions reduces the metastable population. In many cases, the ion beam can be made to consist almost only of ground state ions, permitting unambiguous comparisons with theory.

Here, for Fe^{8+}, the storage time achievable with present technology was not adequate to completely eliminate all of the metastable levels. Nevertheless, storing the ions greatly reduces the number of contributing levels and makes a comparison with theory tractable, even if not wholly unambiguous. The influence of metastables on our results is described in detail in below, in section 3.

Here we present measurements of electron impact ionization (EII) for Ar-like Fe^{8+} forming Cl-like Fe^{9+}. We measured the single ionization cross section from 120 eV up to 1200 eV. This includes the following direct ionization channels:

$$e^- + \mathrm{Fe}^{8+}(2s^2\,2p^6\,3s^2\,3p^6) \rightarrow \begin{cases} \mathrm{Fe}^{9+}(2s^2\,2p^6\,3s^2\,3p^5) + 2e^- \\ \mathrm{Fe}^{9+}(2s^2\,2p^6\,3s\,3p^6) + 2e^- \\ \mathrm{Fe}^{9+}(2s^2\,2p^5\,3s^2\,3p^6) + 2e^- \\ \mathrm{Fe}^{9+}(2s\,2p^6\,3s^2\,3p^6) + 2e^- \end{cases}. \quad (1)$$

Kramida *et al* [6] give the thresholds for ionization of the 3p and 3s electrons as 233.6 and 269.5 eV, respectively. The thresholds for direct ionization of the 2p and 2s electrons are about 978 and 1094 eV, respectively [7]. However, direct ionization of an electron with principal quantum number $n = 2$ produces an excited state that relaxes through autoionization with a probability $\gtrsim$90%. This leads to a net double ionization rather than single ionization. Excitation-autoionization (EA) forming Fe^{9+} is also predicted to contribute to the cross section through the excitation of $n = 2$ electrons above 650 eV [8–10].

2. Experimental method and analysis

Our cross section measurements were performed using the TSR heavy ion storage ring [11, 12] located at the Max-Planck-Institut für Kernphysik in Heidelberg, Germany. The procedures used here are basically the same as those we have described for previous EII measurements and are described in detail in [13–21]. Recombination measurements for Fe^{8+} were previously performed at TSR by [22], who used similar methods. Since the procedures have already been described extensively, we mention here only a few relevant details.

A beam of $^{56}Fe^{8+}$ ions was injected into TSR with an energy of 82.1 MeV. The injection of the ions was done in a series of six pulses spaced 1.47 s apart. After this series of pulses, the ions were stored for 15 s before the measurements started. This waiting time allowed all but a few metastable levels to radiatively relax to the ground level prior to data collection. During this time the ions were merged with a co-propagating electron beam, called the Cooler. The electron beam energy was set to a value suitable for electron cooling, i.e., corresponding to zero average collision energy with the circulating ions [23]. After this initial cooling time, electron–ion collisions were studied at various collision energies by changing the electron beam energy. The ionized or recombined products of any electron–ion collisions in the interaction region were separated from the parent beam by a dipole magnet and directed onto charged-particle counting detectors, one for ionization measurements and the other for recombination. Background count rates were obtained by collecting a reference signal at a fixed relative energy, which was set below the ionization threshold for collision energies up to 860 eV. Due to technical limitations, for collision energies above 860 eV, the reference energy could not be set so far away from the measurement energy and so the reference signal at those energies is not purely background. The correction to the background signal in these cases has been described in detail in our previous work (e.g., [16]).

Table 1. Sources of uncertainty.

Source	Estimated 1σ uncertainty
Counting statistics	2%
Detector efficiency	3%
Electron density	3%
Ion current measurement	15%
Quadrature sum	16%

The background rate was subtracted from the count rate at the measurement energy and normalized in order to obtain the EII cross section, as has been described previously [15]. The uncertainties in the measurement are summarized in table 1. These uncertainties include an uncertainty of about 3% from the detector efficiency [24] and about 3% from the electron density [25]. The largest uncertainty is from the ion current, which was measured using a beam profile monitor [26]. The calibration of this device fluctuates over time and must be periodically reestablished. In this case we estimate that the calibration was accurate to about 15%, leading to a corresponding 15% uncertainty in the EII cross section. In some previous work, we have applied a correction to account for energy dependent changes in the pressure, which modifies the background rate due to stripping and electron capture from the residual gas in the ring [14]. Here we found no significant pressure variation, and so we omit this correction. The cross section was corrected for the influence of the merging and demerging sections of the Cooler where the ion and electron beams are not co-linear by using the method of [27].

3. Metastables

Metastable levels in the ion beam have been a significant problem in systems isoelectronic to Fe^{8+}, such as in the measurements of Ti^{4+} [28], Cr^{6+} [29], and Ni^{10+} [30]. The measurement of the isoelectronic ion Mn^{7+} by [31] does not contain an obvious signal from metastables, but Dere [10] found that the cross section was much larger than predicted by theory and so considered the cross section to be unreliable. For neutral Ar and K^+ the existing EII measurements do not show evidence for significant metastable contamination. For Ar, this is because it is a neutral cold gas and so the

metastable levels were not populated. For the K^+ measurements, the ions were produced using a heated surface at which the thermal energy is too small to excite the metastable levels [32–34].

Although our storage ring measurement has, in the case of Fe^{8+}, been unable to completely eliminate metastables from the beam, the long storage time does reduce the number of problematic metastables to only a few levels. In the following, the discussion of lifetimes is based on the calculations of [35–37], which are tabulated in the CHIANTI atomic database [38]. The Fe^{8+} ground level is $3p^6\ ^1S_0$. The first excited level is $3p^5\,3d\ ^3P_0$, which lies 50.3 eV above the ground level. This level cannot decay to the ground level through a single photon transition, but instead the dominant channel is through an E1M1 two photon decay. As a result, it has an essentially infinite lifetime. In previous work, such metastables were removed using hyperfine-induced transitions [17, 39], but no hyperfine splitting exists for ^{56}Fe, as the nuclear spin is zero. The next important metastable level is the $3p^5\,3d\ ^3F_4$ level at 52.8 eV, which has a predicted lifetime of 970 s. Because this is much longer than the TSR storage time, the metastables cannot be removed from the beam by delaying the measurements. The $3p^5\,3d\ ^3F_3$ level at 53.2 eV is also metastable, but with a significantly shorter lifetime of about 0.9 s. We expect that this last level is removed in our experiment, but it is important because it decays primarily into the $^3F_4$ level. Other metastable levels of the $3p^5\,3d$ configuration are also predicted to have shorter lifetimes, for example the $^3F_2$ at 0.2 s, $^1D_2$ at 0.01 s, and $^3P_2$ at 0.01 s. These and all other initially excited levels are expected to decay before data collection begins.

3.1. Simulated level population

We have used several methods to estimate the metastable fraction in the ion beam. First, we have modeled the relative level populations over time as described in [40]. We initialized the simulation with a Boltzmann distributed population at $k_BT = 87$ eV, where k_B is the Boltzmann constant and T is the temperature. This is an estimate of the effective temperature of the electrons when the ions are produced in the stripping foil. Energy levels and radiative electromagnetic decay rates for all the excited Fe^{8+} levels were taken from the tabulated values of [38] and the populations were tracked using exponentially increasing time steps [40]. For times >0.1 s, figure 1 shows the evolution of the fractional metastable level populations remaining in the stored ion beam for the six-pulse injection scheme used in the experiment, with $t = 0$ corresponding to the end of the last injection. Data collection began at about 15 s and ended at about 50 s, as indicated by the vertical dotted lines in the figure. The calculation shows that the infinite-lifetime $^3P_0$ level is predicted to have a population of less than 2%. The most important metastable level is the $^3F_4$ level, which increases in population initially due to radiative decays from the $^3F_3$ level. From these simulations, we estimate that the beam would be about 43% ground level ions and 57% metastables during the data collection period.

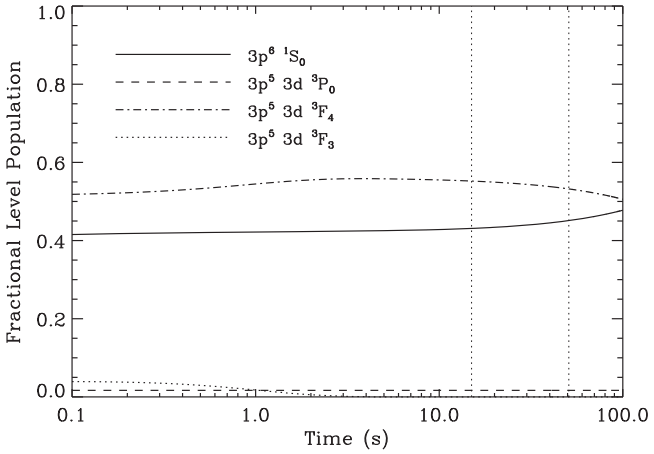

Figure 1. Modeled level populations for the ground level $3p^6\ ^1S_0$ and the long-lived $3p^5\,3d$ metastable levels. The model assumes an initial Boltzmann distribution with $k_BT = 87$ eV and accounts for the injection scheme used in the experiment, with $t = 0$ representing the time of the last ion injection into TSR. Data collection began at $t = 15$ s and ended at $t \approx 50$ s. This time interval falls within the vertical dotted lines in the figure. All levels other than the three appearing in the figure have decayed within the first 0.1 s.

3.2. Comparison with theoretical cross sections

An alternative method for estimating the metastable fraction is to compare the measured EII cross section to the predicted cross sections from the ground and metastable levels. Here, we will neglect the $^3P_0$ level, since above we predicted its population to be small compared to that of the $^3F_4$ level. Then the total cross section is given by

$$\sigma_{I,tot} = f_m\,\sigma_{I,m} + (1 - f_m)\sigma_{I,g}, \qquad (2)$$

where f_m is the metastable fraction and $\sigma_{I,m}$ and $\sigma_{I,g}$ are the cross sections for ionization from the metastable and ground levels, respectively.

Theoretical cross sections for ionization from both the ground configuration and from the metastable $3p^5\,3d$ configuration were previously given by [8]. Those calculations included direct ionization from all of the $n = 3$ levels and EA for $3s - 4l$ transitions for the metastable configuration. Considering first the ground configuration, the $3s - nl$ transitions with $n \geqslant 6$ can also autoionize, but this was not included in [8]. Thus, we have extended those calculations for the ground level by performing a new configuration averaged distorted wave (CADW) calculation that includes the $3s - nl$ EA channels for $n = 6$–10. Considering next the metastable ions, we have mainly relied on the previous calculations of Pindzola *et al* [8]. However, as we expect that the metastable population of the ion beam is dominated by the $^3F_4$ level, we have recalculated the direct ionization calculation from that level only rather than using the previous configuration averaged results. For this direct ionization contribution, we found negligible difference between our new results and those of Pindzola *et al* [8]. In order to include the indirect (i.e., EA) contribution from this level, would require more complex calculations that would incorporate a detailed study of the convergence for various n and l levels. That analysis is

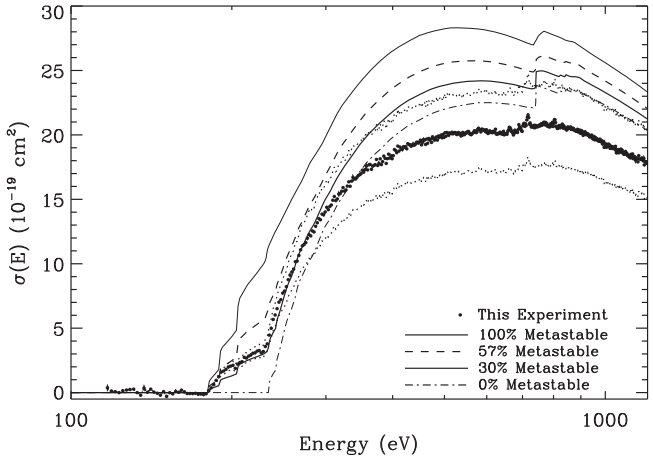

Figure 2. Filled circles show the measured Fe^{8+} EII cross section and the thin dotted curves indicate the systematic uncertainties. The other curves indicate the cross section for different fractions of the $3p^6$ 3d metastable configuration using the theoretical predictions of Pindzola *et al* [8] and our new CADW calculations for the ground level (see text for details). These fractions range from 100% metastables (dashed–dotted–dotted–dotted curve); to 57% metastables (dashed curve), corresponding to the fraction given by the radiative decay model; to 30% metastables (solid curve), which is the best fit found by comparing theory to experiment; to 0% metastables (dashed–dotted curve).

beyond the scope of this paper, and so a revision of the indirect contributions is omitted here.

We have compared our cross section measurements to the results of these calculations in order to estimate the metastable fraction during the experiment. Figure 2 shows the measured ionization cross section compared to the calculations with four different values of f_m. Values of $f_m = 0\%$ and $f_m = 100\%$ are illustrated by the dashed–dotted and dashed–dotted–dotted–dotted curves, respectively.

There is clearly a large contribution to the experimental cross section from metastables, as can be seen by the presence of a significant cross section below the ground level threshold of 233.6 eV. Using equation (2), we performed a least squares fit to find the value of f_m that best fits the measured cross section and found that $f_m = 30 \pm 3\%$. This value depends on the energy range over which theory and experiment are compared, which is the main contribution to the uncertainty quoted here. (There is also an unquantified uncertainty arising from the accuracy of the theoretical calculations.) The thin dotted lines in the figure indicate the systematic uncertainties on the total experimental measurement. With $f_m = 30\%$, the theoretical cross section falls mostly within these uncertainties below 300 eV and slightly outside the uncertainties at higher energies. A problem with this method of quantifying the metastable fraction is that it implicitly assumes that the theory is correct. The ability of the experiment to provide a verification of the calculations is reduced, because the data are being interpreted using the theory itself.

For comparison, the dashed line in figure 2 illustrates the predicted cross section if $f_m = 57\%$, which is the fraction predicted based on the radiative decay model discussed above. This prediction results in a cross section that differs from the experiment outside of the uncertainties. This might indicate that the calculation based on radiative decay rates is in error, possibly because some of the decay rates are underestimated or because the initial level populations are not well described by a Boltzmann distribution. Alternatively, it is possible that the radiative decay calculation is roughly correct, but that the discrepancy lies with inaccuracy in the theoretical cross sections.

3.3. Metastable and ground-level beam lifetimes

We have also measured the lifetimes of the ground and metastable portions of the ion beam. In order to do this, we measured the ionization and recombination count rates at two different collision energies as a function of time. One energy was set to 116 eV, which is below the ionization threshold for both the metastables and the ground level. The other energy we used was 201 eV, which is above the threshold for ionization of the metastables, but below the threshold for ground level ions. At the lower energy point, the measured count rate R_{lo} is due to electron stripping by both ground level and metastable ions off the residual gas in the vacuum system

$$R_{lo} = C_{m,gas}N_m + C_{g,gas}N_g. \quad (3)$$

Here N_m and N_g are the number of metastable and ground-level ions in the beam. The constants $C_{m,gas}$ and $C_{g,gas}$ describe the rate of stripping collisions between the ions and the residual gas. These depend on the collision cross section, residual gas density, interaction length, and ion velocity, all of which are constant since the ions have a fixed energy of 82.1 MeV. The interaction length here is greater than that for electron–ion collisions, since collisions with the residual gas can occur along the entire ~10 m leg of the TSR upstream of the detector. At the higher energy, the count rate includes ionization from stripping and also some additional counts from EII of the metastables

$$R_{hi} = C_{m,gas}N_m + C_{g,gas}N_g + C_{m,e}N_m = R_{lo} + C_{m,e}N_m, \quad (4)$$

where $C_{m,e}$ is proportional to the EII cross section, the electron density in electron beam, and the length of the interaction region. Note that $R_{hi} - R_{lo} \propto N_m$.

Losses from the ion beam are caused by collisions with the residual gas anywhere in the ring and by electron–ion collisions in the Cooler. Residual gas collisions can cause losses through stripping, electron capture, and scattering, which moves an ion trajectory out of the storage phase space. Compared to losses from gas collisions, the losses from electron–ion collisions are negligible. At these energies, R_{hi} is only about 10% larger than R_{lo}, indicating that most counts are due to stripping with little contribution from EII. Although we do not discuss recombination in detail here, the recombination count rates were also not very different between these two energies. This implies that that most recombination counts come from electron capture off the residual gas or that the electron–ion recombination rate does not vary between these two collision energies. A more detailed analysis of loss rates has been presented by Schippers *et al* [39].

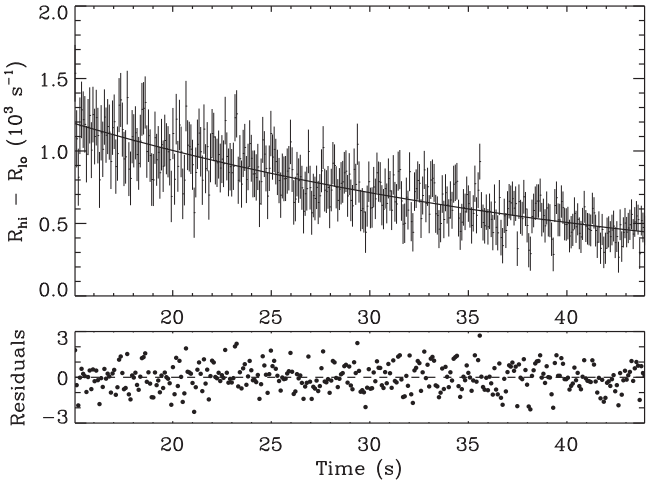

Figure 3. Symbols with error bars show the difference in the count rate on the ionization detector at the energies 201 eV (hi) and 116 eV (lo) as a function of time. The solid line illustrates a single exponential fit to this decay. The residuals are plotted in the lower panel, and imply that a single exponential does fit these data. The fitted decay rate is $0.034 \pm 0.001\ s^{-1}$ and reflects the loss of metastable ions from the beam.

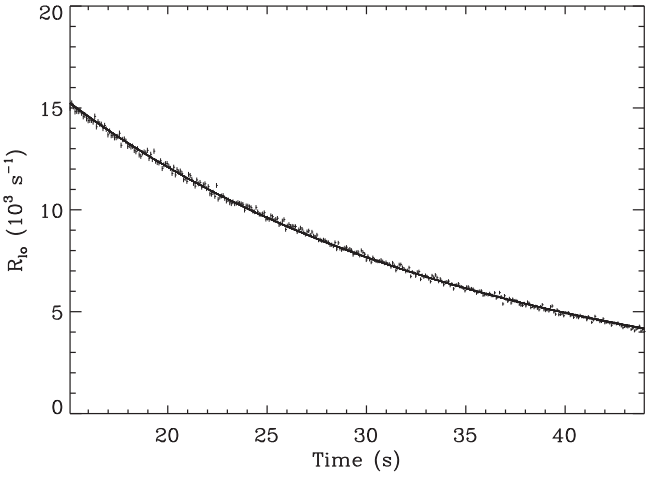

Figure 4. The symbols indicate the count rate on the ionization detector at a collision energy of 116 eV, below the ionization threshold for either ground or metastable ions. Thus, these counts come from collisions with the residual gas in the vacuum system. The vertical lengths of the symbols show the 1σ statistical uncertainties on each point. The solid curve is a fit to the data that is the sum of two exponentials. The part of the decay due to metastable losses is fixed at $0.034 \pm 0.001\ s^{-1}$. Fitting determines the loss rate for ground level ions to be $0.061 \pm 0.002\ s^{-1}$ (see text for details).

Electron–ion collisions are actually much less important than the above 10% estimate based on the detector count rates suggests. This is because electron–ion collisions occur only over a 1.5 m section of TSR, whereas residual gas collisions occur over the entire 55.4 m circumference of TSR. Taking into account the ≈0.03 ratio of these length scales, electron–ion collisions cause less than 0.3% of the beam losses and can be neglected.

The number of metastable ions in the ring then changes according to

$$\frac{dN_m}{dt} = -(A_{m,g} + A_{m,gas})N_m, \tag{5}$$

where $A_{m,g}$ is the total decay rate, radiative and collisional, from the metastable level to the ground level and $A_{m,gas}$ is the loss rate from charge-changing and scattering collisions with the residual gas. The above expression neglects collisional excitation from the ground level to the metastable level, the justification for which is discussed below. The number of ground level ions changes as

$$\frac{dN_g}{dt} = A_{m,g}N_m - A_{g,gas}N_g. \tag{6}$$

Equation (5) implies that

$$N_m(t) = N_m(0)e^{-(A_{m,g}+A_{m,gas})t}, \tag{7}$$

We can fit an exponential function to $R_{hi} - R_{lo}$ in order to determine the rate $A_m \equiv A_{m,g} + A_{m,gas}$. The resulting fit is shown in figure 3. Note that a single exponential decay provides a very good fit, as can be seen in the residuals in the lower panel of figure 3. This provides some justification for our neglect of collisional excitation from the ground level; although given the uncertainties, collisional excitation cannot be ruled out. If such excitation were important, $N_m(t)$ would depend on $N_g(t)$ and would require a multiple exponential fit. From the fit, we found $A_m = 0.034 \pm 0.001\ s^{-1}$, which corresponds to a storage lifetime of about 29 s.

From equations (6) and (7) we find that

$$N_g(t) = c_1e^{-A_m t} + c_2e^{-A_{g,gas}t}, \tag{8}$$

where c_1 and c_2 are parameters that are constant in time and depend on the initial ground and metastable level populations. Their values are not important here, because we are only interested in loss rates. Both R_{lo} and R_{hi} are then just a sum of two exponentials, with one following a decay rate A_m and the other $A_g \equiv A_{g,gas}$. In order to determine the value of A_g, we performed a fit using a sum of two exponential decays to the data for R_{lo} and R_{hi}. Since the value of A_m has already been determined, this value is fixed. There are then three parameters for the fit, a proportionality constant for each exponential term and the rate A_g. The uncertainty on A_m was propagated into the uncertainty on the fitted value for A_g by performing the fit 2000 times and taking the fixed value A_m from a normal distribution with mean and standard deviation equal to the values given above. An example of the fit for R_{lo} is given in figure 4. We found $A_g = 0.061 \pm 0.002$, or a storage lifetime of about 16 s.

These results suggest that the storage lifetime of the metastables in the ion beam is actually longer than that of the ground level ions. This is in contrast to what is expected from the slow radiative decays of the metastable levels to the ground level. It is also unexpected considering that a more loosely bound electron in a metastable level can be striped off more easily than a tightly bound one in the ground level. One possible explanation is that the cross section for collisions between the ground level ions and the residual gas is larger than for the metastables, though the precise loss process that

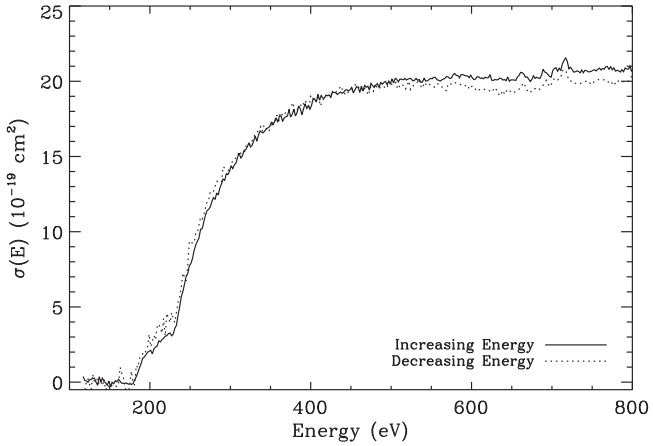

Figure 5. EII cross section for Fe^{8+} obtained from energy scans conducted with the energy increasing over time from low to high energy (solid curve) compared to that obtained from scans with the energy decreasing with storage time from high to low energy (dotted curve). These results suggest that the metastable fraction of the ion beam increases during the course of the experiment by a factor of about 1.3.

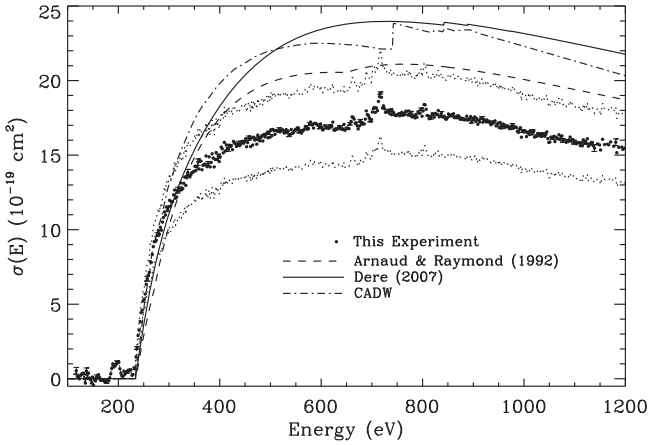

Figure 6. EII cross section for Fe^{8+} (filled circles) corrected by subtracting an estimated 30% metastable contribution. The dotted curves illustrate the 1σ systematic uncertainties due to the ion current measurement. The total systematic uncertainties are larger and unquantifiable due to the uncertainties associated with the metastables. Statistical uncertainties are indicated by the error bars on selected points. The dashed curve illustrates the cross section from Arnaud and Raymond [9], the solid curve shows the cross section given by Dere [10], and the dashed–dotted curve indicates our updated CADW calculations.

would lead to the different beam lifetimes is unclear. Alternatively, it may be that collisional excitation from the ground state populating the metastable level is important. Since we know that residual gas collisions lead to ionization through stripping, we expect that some degree of excitation from the ground to the metastable level should also occur. The effects of this excitation might be reduced by collisional deexcitation. In view of all the various simultaneous effects to be considered, our data are insufficient to quantify these rates.

A slower decay rate for the metastables as compared to the ground level ions implies that the fraction of metastables in the beam is increasing over time. A typical energy scan of the ionization cross section lasted for about 30 s in this experiment. Given the above lifetimes, the metastable fraction would increase by a factor of about 1.4 over this time. Assuming that the initial metastable fraction at the end of the cooling period is 30%, the metastable fraction at the end of the measurement cycle would be 42%.

There is evidence that the metastable fraction grows during the measurement in the cross sections themselves. Figure 5 shows the EII cross section derived from energy scans progressing in opposite directions. The solid curve shows the result obtained from scans with increasing energy over time, which was the precedure used for all other parts of our analysis. The dotted curve illustrates the results from a test run where the energy was decreasing over time during the energy scan. We find that at low energies the cross section in the decreasing energy scan is greater but that at high energies the cross section for the scan with increasing energy is greater. This is consistent with the metastable fraction increasing during data collection. The cross section for EII from the metastable level is calculated to be greater than that for the ground level and so the increasing metastable fraction causes the cross section measured towards the end of data collection to be larger due to the larger fraction of metastables. Quantitiatively, we find that the integrated cross section between the metastable EII threshold and the ground state threshold is a factor of $\approx$1.3 larger for the scan with decreasing energy compared to those with increasing energy. This implies a factor of 1.3 increase in the metastable fraction during data collection, which is roughly consistent with the value of 1.4 that we would expect based on the beam lifetime analysis.

To summarize, the metastables in this experiment are problematic in two ways. First, the measured cross section is the sum of a ground state and a metastable cross section. This makes the interpretation of the cross section ambiguous without an accurate estimate of f_m. The second issue, is that it appears that f_m is increasing by a factor of about 1.3 during the measurements. This results in some distortion to the measured cross section. We expect that the only significant metastable level contribution to be from the $^3F_4$ level, which we estimate varies from $f_m \approx 0.3$ up to ≈ 0.4 in the beam during the measurement. Since we lack a more precise value, we estimate the uncertainty in the cross section due to the metastables taking a constant value of $f_m = 0.3$.

4. Cross section

Figure 6 shows the estimated ground level EII cross section for Fe^{8+}. The filled circles in figure 6 show the experimental results, which have been corrected to remove, as far as possible, the contribution of the metastables. For this correction, we have assumed a 30% metastable fraction and subtracted 0.3 times our calculation for the theoretical metastable cross section from the experimental data. Then the resulting cross section was rescaled by multiplying by a factor of $1/(1-0.3)$ to obtain the estimated cross section for

ionization from the ground level. The small dotted curves indicate the systematic uncertainties due to the ion current measurement and the error bars illustrate the statistical uncertainties. Because the uncertainties associated with the metastables are large and difficult to quantify, the actual systematic errors are larger than implied in the figure.

We compare our experimental results to several theoretical predictions. The dashed curve in figure 6 shows the recommended cross section of Arnaud and Raymond [9], which is based on the calculations of Younger [41] and Pindzola *et al* [8]. The solid curve illustrates the cross section calculated by Dere [10] and the dotted–dashed curve is our present CADW calculation. All of the theory curves lie above the experimental result by ≈15%–40% over the measured range. This may indicate that theory overestimates the EII cross section. An alternative explanation is that the estimated metastable fraction is different from 30%, which would also imply some inaccuracy in the theory for the metastable EII cross section that formed the basis for this value of the metastable fraction.

One detail that can be seen, is the presence in our measured cross section of an EA contribution at about 650 eV. This is most likely due to excitation from the $n = 2$ level to the 3d level [8] and is included in [9], however the channel was omitted from the calculations of [10]. Those calculations did, however, include EA from excitations from $n = 2$ to $n = 4$ and 5, but we find those contributions to be very small as we do not clearly detect them in the experiment.

We have found previously that EA contributions from $n = 3$ excitations are important for other Fe ions with a $3s^2\ 3p^q$ configuration L-shell Fe ions [15, 16, 18, 19], and this is also true here. In figure 6 the effect of this EA channel can be seen near the ionization threshold, where the present CADW cross section increases more rapidly than either the Arnaud and Raymond [9] or Dere [10] cross sections. The CADW calculation includes $3s - nl$ EA for $n = 6$–10. These EA channels are omitted from [9]. Dere does include $3s - 4l$ and $3s - 5l$ channels, but these are below the ionization threshold and do not contribute to the cross section. With the addition of the $3s - nl$ channels for $n = 6$–10, our new theoretical calculation better matches the slope of the measured cross section near the ground state ionization threshold. However, more detailed calculations are still needed, because we have assumed here a branching ratio of unity for all of the EA channels and therefore likely overestimate the contribution from 3s EA.

5. Summary and outlook

We have measured the EII cross section for Fe^{8+} forming Fe^{9+} using the TSR ion storage ring. For this ion, the $3p^5\ 3d\ ^3F_4$ metastable level has a long lifetime and could not be removed by storing the ions in TSR. Based on an estimate using theoretical predictions for the metastable cross section, we estimated that the metastable fraction was ∼30% at the start of measurements. However, ground level ions appear to be removed from the beam preferentially so that the metastable fraction actually grows during measurement. As a result, the metastable fraction for portions of the measurement could then be as large as 42%.

Our measurements suggest several discrepancies between experiment and the theoretical calculations that are most commonly used in the analysis of astrophysical spectra [9, 10]. First, we find that the 2–3 EA channel is present in the measurement, as predicted by [8] and should not be omitted from calculations. Second, $3s - nl$ EA channels appear to be necessary to match the slope of the measurement near the ground state ionization threshold. Finally, the overall magnitude of the ground level EII calculations may overestimate the cross section, although this inference is especially sensitive to the metastable fraction and other systematic uncertainties.

A more detailed and less ambiguous comparison with theory could be performed by reducing the large metastable fraction in the ion beam. In order to remove the metastables, it is necessary to store the ions for a long enough time, ∼1000 s, so that the $^3F_4$ level could radiatively decay to the ground level. At the same time, collisions with the residual gas need to be avoided because such collisions appear to increase the fraction of metastables relative to ground level ions and because they reduce the overall beam lifetime.

These conditions may be met using the cryogenic storage ring (CSR) currently being commissioned at the Max-Planck-Institut für Kernphysik [42, 43]. CSR is cooled using liquid helium to below 10 K so that the whole vacuum chamber operates as a cryopump. The resulting residual gas density is $<10^3$ cm^{-3}, which permits beam lifetimes of $\gtrsim 10^3$ s. A new cryogenic particle detector system has also been developed that will be suitable EII and recombination measurements [44].

Future measurements of Fe^{8+} EII using CSR may resolve the problem with metastables in the ion beam and obtain unambiguous EII data for this ion. Such data are needed as there are currently no measurements for EII of Ar-like ions from charge states higher than singly ionized potassium that are not affected by significant metastable fractions [10].

Acknowledgments

We appreciate the efficient support by the MPIK accelerator and TSR groups during the beamtime. This work was supported in part by the NASA Astronomy and Physics Research and Analysis program and the NASA Solar Heliospheric Physics program. We also acknowledge financial support by the Max-Planck-Gesellschaft, Germany and from Deutsche Forschungsgemeinschaft (contract no. Schi 378/8-1).

References

[1] Bryans P, Landi E and Savin D W 2009 *Astrophys. J.* **691** 1540
[2] Young P R 2009 *Astrophys. J.* **691** 77–81
[3] Young P R and Landi E 2009 *Astrophys. J.* **707** 173–92
[4] O'Dwyer B, Del Zanna G, Mason H E, Weber M A and Tripathi D 2010 *Astron. Astrophys.* **521** 21

[5] Beiersdorfer P, Lepson J K, Desai P, Díaz F and Ishikawa Y 2014 *Astrophys. J. Suppl. Ser.* **210** 16
[6] Kramida A, Ralchenko Y, Reader J and NIST ASD Team 2013 *Nist Atomic Spectra Database (Version 5.1)* National Institute of Standards and Technology (http://physics.nist.gov/asd)
[7] Kaastra J S and Mewe R 1993 *A&AS* **97** 443
[8] Pindzola M S, Griffin D C, Bottcher C, Younger S M and Hunter H T 1987 *Nucl. Fusion Spec. Suppl.* **1987** 21
[9] Arnaud M and Raymond J 1992 *Astrophys. J.* **398** 394
[10] Dere K P 2007 *Astron. Astrophys.* **466** 771
[11] Habs D *et al* 1989 *Nucl. Instrum. Methods* B **43** 390
[12] Grieser M *et al* 2012 *Eur. J. Phys.* **207** 1–17
[13] Linkemann J, Müller A, Kenntner J, Habs D, Schwalm D, Wolf A, Badnell N R and Pindzola M S 1995 *Phys. Rev. Lett* **74** 4173
[14] Hahn M, Bernhardt D, Lestinsky M, Müller A, Novotný O, Schippers S, Wolf A and Savin D W 2010 *Astrophys. J.* **712** 1166
[15] Hahn M *et al* 2011 *Astrophys. J.* **729** 76
[16] Hahn M, Grieser M, Krantz C, Lestinsky M, Müller A, Novotný O, Repnow R, Schippers S, Wolf A and Savin D W 2011 *Astrophys. J.* **735** 105
[17] Hahn M *et al* 2012 *Phys. Rev.* A **85** 042713
[18] Hahn M *et al* 2012 *Astrophys. J.* **760** 80
[19] Hahn M *et al* 2013 *Astrophys. J.* **767** 47
[20] Hahn M *et al* 2015 *Astrophys. J.* **813** 16
[21] Bernhardt D *et al* 2014 *Phys. Rev.* A **90** 012702
[22] Schmidt E W *et al* 2008 *Astron. Astrophys.* **492** 265–75
[23] Poth H 1990 *Phys. Rep.* **196** 135
[24] Rinn K, Müller A, Eichenauer H and Salzborn E 1982 *Rev. Sci. Instrum.* **53** 829
[25] Lestinsky M *et al* 2009 *Astrophys. J.* **698** 648
[26] Hochadel B, Albrecht F, Grieser M, Schwalm D, Szmola E and Wolf A 1994 *Nucl. Instrum. Methods* A **343** 401
[27] Lampert A, Wolf A, Habs D, Kenntner J, Kilgus G, Schwalm D, Pindzola M S and Badnell N R 1996 *Phys. Rev.* A **53** 1413
[28] Hartenfeller U, Aichele K, Hathiramani D, Hofmann G, Schäfer V, Steidl M, Stenke M, Salzborn E and Pindzola M S 1998 *J. Phys. B: At. Mol. Opt. Phys.* **31** 2999
[29] Sataka M, Ohtani S, Swenson D and Gregory D C 1989 *Phys. Rev.* A **39** 2397
[30] Cherkani-Hassani S, Khouilid M and Defrance P 2001 *Phys. Scr.* **T92** 287
[31] Rejoub R and Phaneuf R A 2000 *Phys. Rev.* A **61** 032706
[32] Hooper J W, Lineberger W C and Bacon F M 1966 *Phys. Rev.* **141** 165
[33] Peart B and Dolder K T 1968 *J. Phys. B: At. Mol. Phys.* **1** 240
[34] Hirayama T, Oda K, Morikawa Y, Ono T, Ikezaki Y, Takayanagi T, Wakiya K and Suzuki H 1986 *J. Phys. Soc. Japan* **55** 1411–4
[35] Storey P J, Zeippen C J and Le Dourneuf M 2002 *Astron. Astrophys.* **394** 753
[36] Landi E and Young P R 2009 *Astrophys. J.* **707** 1191
[37] O'Dwyer B, Del Zanna G, Badnell N R, Mason H E and Storey P J 2012 *Astron. Astrophys.* **537** 22
[38] Landi E, Young P R, Dere K P, Del Zanna G and Mason H E 2013 *Astrophys. J.* **763** 86
[39] Schippers S *et al* 2012 *Phys. Rev.* A **85** 012513
[40] Lestinsky M *et al* 2012 *Astrophys. J.* **758** 40
[41] Younger S M 1983 *J. Quant. Spectrosc. Radiat. Transfer.* **29** 61
[42] Krantz C *et al* 2011 *J. Phys. Conf. Ser.* **300** 012010
[43] von Hahn R *et al* 2011 *Nucl. Instrum. Methods* B **269** 2871
[44] Spruck K *et al* 2015 *Rev. Sci. Instrum.* **86** 023303